DOA Estimation of Coherent Signals based on EPUMA Method with Frequency Beam Scanning Leaky-Wave Antennas

Diyuan Xu, Yide Wang, Julien Sarrazin, Biyun Ma, Qingqing Zhu

Date of publication xxxx 00, 0000, date of current version xxxx 00, 0000.

Digital Object Identifier 10.1109/ACCESS.2022.0122113

DOA Estimation of Coherent Signals based on EPUMA Method with Frequency Beam Scanning Leaky-Wave Antennas

DIYUAN XU[1], YIDE WANG[2], (Senior Member, IEEE), JULIEN SARRAZIN[3], (Senior Member, IEEE), BIYUN MA[1], and QINGQING ZHU[1]

[1]School of Electronics and Information Engineering, South China University of Technology, 510640 Guangzhou, China (e-mail: eebyma@scut.edu.cn)
[2]Institut d'Electronique et des Technologies du NumeRique (IETR), CNRS UMR6164, Nantes University, 44306 Nantes, France (e-mail: yide.wang@univ-nantes.fr)
[3] Laboratoire de Génie Electrique et Electronique de Paris, CNRS, Sorbonne Université, 75252, Paris, France; CentraleSupélec, CNRS, Université Paris-Saclay, 91192, Gif-sur-Yvette, France
(e-mail:julien.sarrazin@sorbonne-universite.fr)

Corresponding author: Biyun MA (e-mail: eebyma@scut.edu.cn).

This work was supported by the ANR BeSensiCom project, grant ANR-22-CE25-0002 of the French Agence Nationale de la Recherche, Natural Science Foundation of Guangdong Province of China under Grant No.2021A1515011854, 2021A1515011842, 2022A1515011830, 2023A1515011420, and carried out in the framework of COST Action CA20120 INTERACT.

ABSTRACT A technique to estimate the DOAs of coherent sources using a passive frequency-beam scanning leaky-wave antenna (FBS-LWA) with a subspace based method is presented. To do so, a combination of enhanced principal-singular-vector utilization for modal analysis (EPUMA) algorithm and linear interpolation technique is proposed. The simulation results show the effectiveness of the proposed method for DOA estimation of multiple coherent signals with hyper-resolution capabilities. With respect to classical antenna arrays, such FBS-LWAs reduce system complexity since only one radio-frequency receiver is required to perform DOA estimation in one angular plane.

INDEX TERMS Frequency scanning leaky-wave antenna; interpolation; EPUMA; coherent signals

I. INTRODUCTION

The estimation of directions-of-arrival (DOAs) of incoming sources is important in many applications such as radar, sonar, and telecommunications. Conventional DOA estimation systems require a large number of mutually independent radio frequency (RF) channels, including antenna sensors, RF down-conversion, signal processing modules, etc. [1]. It is a continuous trend to simplify the hardware implementation [2].

Leaky-wave antennas (LWAs) have gained significant attention in academia and industry since their introduction in the 1940s [3]. These antennas are based on waveguide that supports the propagation of a fast-traveling wave which leaks into the free space in such a way to radiate a directional beam whose angular direction depends on the frequency [4]. So, by using a single-port excitation only and by varying the frequency, the LWA beam can be steered across a field of view (FoV) whose angular range depends on the LWA scanning velocity and the frequency bandwidth over which the system operates. Therefore, unlike phased arrays, LWAs achieve beam scanning without the requirement for complex feeding networks or any active components, such as phase shifters, making them more cost-effective and easier to manufacture [3], [5].

For sensing applications, the spectrum of the signal received by the LWA can be used to estimate DOAs [6]. However, to cover a sufficiently large FoV, the frequency beam scanning leaky-wave antennas (FBS-LWAs) require the signals whose DOAs are to be estimated to be wide-band enough, which jeopardizes the interest in the scheme for many applications. This is why, most of the literature dealing with LWA-based DOA estimation considers electronically-controlled beam scanning LWAs [7], [8]. However, in addition to having more complex structures than FBS-LWAs, such electronically-controlled

LWAs steer their beam sequentially to perform DOA estimation which brings additional constraints on the system (e.g., limited real-time capabilities, waveform duration of the sources...). On the other hand, considerable efforts have been done to achieve fast scanning LWA in order to perform FBS-LWA-based DOA estimation with reduced frequency bandwidth [1], [9]–[14]. In [1], [10]–[12], the received power spectrum is measured to estimate DOAs based on amplitude monopulse radar techniques. Subspace based methods, such as MUSIC, have also been applied with FBS-LWA to estimate DOAs [9], [13], [14]. While these methods achieve hyper-resolution, they fail to retrieve DOAs of coherent sources and therefore perform poorly in multipath environments [15]. To mitigate this issue, subspace techniques require a preprocessing by some decorrelation techniques, e.g., spatial smoothing (SS), modified spatial smoothing preprocessing (MSSP) and Teoplitz reconstruction. These decorrelation techniques need that the steering matrix is a Vandermonde matrix, which is not the case for FBS-LWA due to its frequency scanning characteristics.

Consequently, this paper introduces for the first time, to the best of the author's knowledge, a subspace based method for DOA estimation of coherent sources with FBS-LWA. After transforming the FBS-LWA response matrix to a Vandermonde structure, a modified version of the enhanced principal-singular-vector utilization modal analysis (EPUMA) [16] algorithm is proposed and applied to the FBS-LWA scenario. EPUMA is chosen over MUSIC or ESPRIT because it has a reduced computational complexity and an improved performance, especially for coherent signals and/or small sample scenarios [16], [17]. Note that, the Vandermonde structure is also necessary for the EPUMA algorithm.

Therefore, to address the DOA estimation of coherent signals received by a single-beam FBS-LWA, a novel method is proposed with the following steps. Firstly, the approximate angles of the coherent signals are obtained using the spectrum analysis of the received signals and the single-beam patterns for each frequency of the FBS-LWA and/or beamforming method. Secondly, the steering matrix of the LWA, constructed based on the radiation pattern of the FBS-LWA, is transformed into a virtual Vandermonde matrix using interpolation technique [18]. This transformation allows for the application of decorrelation techniques or EPUMA. Finally, a modified EPUMA algorithm is employed to address the rank-deficient problem arising from multiple coherent signals.

The paper is organized as follows. Section II introduces the signal model including the FBS-LWA model and signal model received by FBS-LWA. Section III describes the interpolation process, which produces a Vandermonde-like FBS-LWA response. Section IV presents the modified EPUMA for multiple coherent signals. Section V shows and discusses some simulation results in different scenarios, and Section VI concludes the paper.

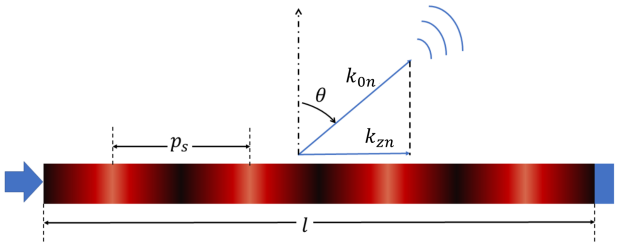

FIGURE 1. 1-D periodic Leaky-wave antenna (input port on the left, matched-load on the right) [9].

II. SIGNAL MODEL

A. LWA MODEL

The LWA model considered in this paper is a single-beam configuration [19], [20], capable of scanning a wide field of view using a wideband signal. A 1-D periodic unidirectional LWA operating on its -1^{th} spatial harmonic is depicted in Figure 1. The theoretical radiation pattern of this antenna at a given frequency f_n can be written as [9]:

$$a_n(\theta) = l e^{-j k_n} \operatorname{sinc}(k_n), n = 1, 2, \ldots, N \quad (1)$$

with $k_n = (k_{zn} - k_{0n} \sin(\theta))\, l/2$, l is the LWA length, $k_{0n} = 2\pi f_n / c$ is the free space wave number with c the light velocity, n represents the n^{th} frequency sample of the operating bandwidth, including N samples between the minimum operating frequency f_{min} and the maximum operating frequency f_{max}. So,

$$\mathbf{f} = [f_{min}, f_{min} + \Delta f, \ldots, f_{max} - \Delta f, f_{max}]^T \quad (2)$$

with $\Delta f = \frac{f_{max} - f_{min}}{N-1}$, f_n the n^{th} element of the frequency vector $\mathbf{f}$. k_{zn} represents the longitudinal wave number inside the guiding structure associated with the -1^{th} space harmonic:

$$k_{zn} = \beta_{0n} - 2\pi/p_s - j\alpha_n, n = 1, 2, \ldots, N \quad (3)$$

where α_n is the attenuation constant, i.e., (6) in [4], accounting for the leakage and the losses of the n^{th} element of the frequency vector $\mathbf{f}$, p_s the spatial period of the geometry modulation of the LWA, β_{0n} the phase constant of the fundamental guided mode. The expression of β_{0n} depends on the guiding structure. Since numerous LWAs of the literature are based on rectangular waveguide technology (see e.g., [3]), its expression is used here for the sake of illustration:

$$\beta_{0n} = k_{0n}\sqrt{\varepsilon_r}\sqrt{1 - (f_c/f_n)^2}, n = 1, 2, \ldots, N \quad (4)$$

where $f_c = \frac{c}{2 W_g \sqrt{\varepsilon_r}}$ is the fundamental mode cutoff frequency, W_g is the width of the waveguide, and ε_r is the relative permittivity of the dielectric filling the waveguide.

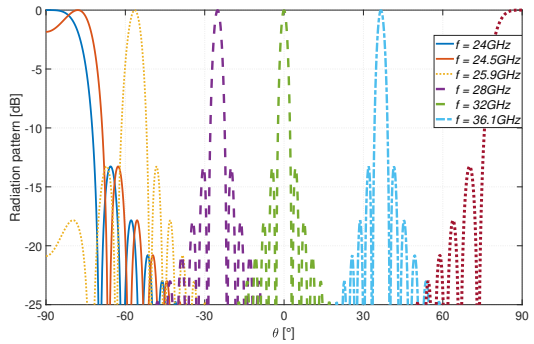

(a) $l = 20$ cm, $\alpha_n/k_{0n} = 0.01$

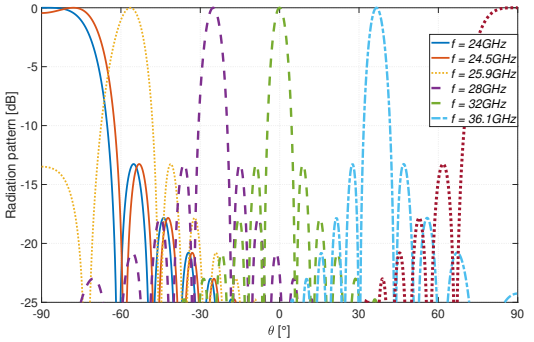

(b) $l = 10$ cm, $\alpha_n/k_{0n} = 0.01$

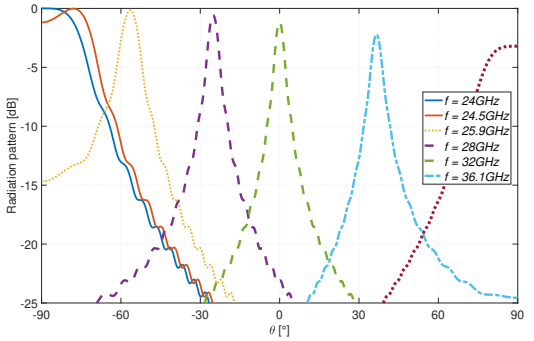

(c) $l = 20$ cm, $\alpha_n/k_{0n} = 0.03$

FIGURE 2. Normalized radiation patterns of different frequencies for FBS-LWA with different lengths

The normalized radiation patterns for some selected frequencies are shown in Figure 2, with the following design parameters, $\varepsilon_r = 10.2$, $W_g = 2.2$ mm and $p_s = 5.4$ mm, $l = 20$ cm and $\alpha_n/k_{0n} = 0.01$ for Figure 2(a), $l = 10$ cm and $\alpha_n/k_{0n} = 0.01$ for Figure 2(b), $l = 20$ cm and $\alpha_n/k_{0n} = 0.03$ for Figure 2(c), respectively. Since only one space harmonic is in the bandwidth from f_{min} to f_{max}, only one main beam is radiated for each frequency f_n, whose angular steering direction scans the whole FoV in the range from f_{min} to f_{max}. This effect is explored in the subsequent sections to perform DOA estimation. It is interesting to observe that the beamwidth of each frequency increases as the length l of the LWA decreases. In addition, compared with Figure 2(a) and Figure 2(c), the ratio of α_n/k_{0n}, which can be controlled by the design of LWA [13], has great effect on the radiation patterns. As the ratio of α_n/k_{0n} increases, the beamwidth of each frequency increases. Practically, a smaller α_n/k_{0n} leads to a bigger LWA aperture with a higher radiation efficiency and a smaller beamwidth for each frequency, which can improve the estimation performance. The influence of the LWA beamwidth will be discussed in section V.

It is important to note that, in practice, for applications involving FBS-LWAs, the data from the radiation patterns obtained through experiments or HFSS simulations are utilized to derive the steering vector $a_n(\theta)$. However, in the subsequent simulations, the steering vector $a_n(\theta)$ corresponding to the radiation pattern of the LWA is obtained using (1) to (4).

B. SIGNAL MODEL RECEIVED BY FBS-LWA

By considering that K DOA signals impinging on the single-beam FBS-LWA with ultrawide-angle frequency beam scanning and high scanning rate, as proposed in [21], from the far field, the following frequency system model can be constructed after fast Fourier transform (FFT) of the received data,

$$\mathbf{y} = \mathbf{A}\mathbf{s} + \mathbf{n} \tag{5}$$

with the received data vector $\mathbf{y} \in \mathbb{C}^{N\times 1}$, the LWA steering matrix $\mathbf{A} = [\mathbf{a}(\theta_1), \mathbf{a}(\theta_2), \ldots, \mathbf{a}(\theta_K)]$, where $\mathbf{a}(\theta) = [a_1(\theta), a_2(\theta), \ldots, a_N(\theta)]^T$, the source vector $\mathbf{s} \in \mathbb{C}^{K\times 1}$, the additive white Gaussian noise (AWGN) vector composed of independent components $\mathbf{n} \in \mathbb{C}^{N\times 1}$ with zero mean and covariance matrix $\sigma^2\mathbf{I}_N$. The columns of $\mathbf{A}$ are the LWA response of incoming plane waves whose DOA is $\theta_{i=1,\ldots,K}$ as described in (1). In addition, it is assumed that $N > K$.

III. SIGNAL MODEL AFTER INTERPOLATION

Based on (1), the steering matrix $\mathbf{A}$ of the FBS-LWA is not a Vandermonde matrix, we should transform it into a Vandermonde matrix to meet the requirements of EPUMA, which relies on linear prediction. To address this challenge, an interpolation based method is introduced in this paper to solve the problem.

Note that, the closer the interpolation directions to the true DOAs of incoming signals, the more accurate the estimation will be. Therefore, firstly, a prior approximate estimation of the DOA is required. Fortunately, the single-beam FBS-LWA is capable of scanning the approximate angular range of signals by the corresponding frequencies of the peaks of the received signal power spectrum and radiation patterns, as depicted in Figure 2, or by beamforming method. It is defined that each sector corresponds to the approximate angular range of a detected signal. Assuming that there are K' sectors successfully detected, where K' represents the number of detected approximate signals, in most cases $K' = K$. However, there are instances where

$K' < K$, indicating that multiple sources are within the same sector. So the sector centers are indicated as $\mathbf{\Theta}_B = [\theta_{B,1}, \theta_{B,2}, \ldots, \theta_{B,K'}]$, corresponding to the K' detected sectors.

Then let $\mathbf{A}_r \in \mathbb{C}^{N \times K_v}$ represent the FBS-LWA virtual steering matrix generated by the K_v virtual directions $\theta_1, \theta_2, \ldots, \theta_{K_v}$, and $K_v > K$. So the K_v virtual directions used to generate the virtual Vandermonde matrix are denoted by

$$\mathbf{\Phi}_v = [\mathbf{\Psi}_{v,1}, \mathbf{\Psi}_{v,2}, \ldots, \mathbf{\Psi}_{v,K'}] \tag{6}$$

The virtual directions are used to represent the information of the real DOAs, but it is also necessary to prevent the virtual directions from interfering with each other. So uniform distribution of virtual directions in each sector is adopted to obtain the K_v virtual directions.

When the virtual directions are uniformly distributed in each sector, a sector will be constructed with $2p+1$ ($p \in \mathbb{N}^+$) points, there are $K_v = K^{'}(2p+1)$ virtual directions in total. And $\mathbf{\Psi}_{v,k} = [\theta_{B,k} - p\delta, \ldots, \theta_{B,k} - \delta, \theta_{B,k}, \theta_{B,k} + \delta, \ldots, \theta_{B,k} + p\delta]$, $k = 1, 2, \ldots, K^{'}$, δ is the interpolation interval. Then,

$$\mathbf{A}_r = \begin{bmatrix} a_1(\theta_1) & \ldots & a_1(\theta_{K_v}) \\ \vdots & \ddots & \vdots \\ a_N(\theta_1) & \ldots & a_N(\theta_{K_v}) \end{bmatrix} \tag{7}$$

where $a_n(\theta)$ is defined in (1). An ideal Vandermonde matrix $\mathbf{A}_l \in \mathbb{C}^{N \times K_v}$ is defined as follows:

$$\mathbf{A}_l = \begin{bmatrix} 1 & 1 & \cdots & 1 \\ e^{j\pi\sin\theta_1} & e^{j\pi\sin\theta_2} & \ldots & e^{j\pi\sin\theta_{K_v}} \\ \vdots & \vdots & \ddots & \vdots \\ e^{j(N-1)\pi\sin\theta_1} & e^{j(N-1)\pi\sin\theta_2} & \ldots & e^{j(N-1)\pi\sin\theta_{K_v}} \end{bmatrix} \tag{8}$$

The interpolation matrix $\mathbf{B}_i \in \mathbb{C}^{N \times N}$ is defined such that [15]:

$$\mathbf{B}_i \mathbf{A}_r = \mathbf{A}_l \tag{9}$$

$\mathbf{B}_i$ can be obtained by the following least squares (LS) solution:

$$\mathbf{B}_i = \mathbf{A}_l \mathbf{A}_r^H \left(\mathbf{A}_r \mathbf{A}_r^H\right)^{-1} \tag{10}$$

So, the relative interpolation error q can be defined as:

$$q = \frac{\|\mathbf{A}_l - \mathbf{B}_i \mathbf{A}_r\|^2}{\|\mathbf{A}_l\|^2} \tag{11}$$

where q is set to be smaller than 10^{-12} to have a good performance.

So the signal $\mathbf{y}$ received by LWA is transformed to the signal $\mathbf{y}_l$, which contains $\mathbf{A}_l^{'} = \mathbf{B}_i \mathbf{A}$ with K real DOAs. Note that, $\mathbf{A}_l$ differs from $\mathbf{A}_l^{'}$ as $\mathbf{A}_l' \in \mathbb{C}^{N \times K}$ and $\mathbf{A}_l \in \mathbb{C}^{N \times K_v}$.

$$\mathbf{y}_l = \mathbf{B}_i \mathbf{y} = \mathbf{A}_l^{'} \mathbf{s} + \mathbf{n}_l \tag{12}$$

where $\mathbf{n}_l = \mathbf{B}_i \mathbf{n}$ is no longer a white noise. Therefore, it is necessary to remove the contribution of $\mathbf{n}_l$. Firstly, the covariance matrix of the received signals, which contains the white noise, is calculated:

$$\mathbf{R} = \mathrm{E}[\mathbf{y}\mathbf{y}^H] = \mathbf{E}_{sr} \mathbf{\Lambda}_{sr} \mathbf{E}_{sr}^H + \sigma^2 \mathbf{I}_N \tag{13}$$

where the columns of $\mathbf{E}_{sr}$ are the eigenvectors associated with the eigenvalues $\mathbf{\Lambda}_{sr} + \sigma^2 \mathbf{I}_{N_r}$, which span the signal subspace. Then the covariance matrix of $\mathbf{y}_l$ is calculated:

$$\begin{aligned} \mathbf{R}_l &= \mathrm{E}[\mathbf{y}_l \mathbf{y}_l^H] = \mathrm{E}[\mathbf{B}_i \mathbf{y} (\mathbf{B}_i \mathbf{y})^H] = \mathrm{E}[\mathbf{B}_i (\mathbf{y}\mathbf{y}^H) \mathbf{B}_i^H] \\ &= \mathbf{B}_i (\mathbf{E}_{sr} \mathbf{\Lambda}_{sr} \mathbf{E}_{sr}^H + \sigma^2 \mathbf{I}_N) \mathbf{B}_i^H \\ &= \mathbf{B}_i \mathbf{E}_{sr} \mathbf{\Lambda}_{sr} \mathbf{E}_{sr}^H \mathbf{B}_i^H + \sigma^2 \mathbf{B}\mathbf{B}_i^H \end{aligned} \tag{14}$$

Finally, the noise contribution in $\mathbf{R}_l$ can be removed as:

$$\mathrm{E}[\mathbf{y}_l \mathbf{y}_l^H] - \sigma^2 \mathbf{B}_i \mathbf{B}_i^H = \mathbf{\Gamma} = \mathbf{E}_{sl} \mathbf{D}_{sl} \mathbf{E}_{sl}^H \tag{15}$$

where $\mathbf{E}_{sl} = [\mathbf{u}_1, \ldots, \mathbf{u}_{N_r}]$ are the eigenvectors associated with the N_r largest eigenvalues in $\mathbf{D}_{sl} = \mathrm{diag}(\lambda_1, \ldots, \lambda_{N_r})$, and span the non zero signal subspace. Since the noise contribution has been removed in (15), theoretically, there will be no noise in the following. N_r is the theoretical rank of the source covariance matrix $\mathbf{\Gamma}_s = \mathrm{E}\left[\mathbf{s}\mathbf{s}^H\right]$, and $N_r < K$ due to the existence of coherent signals. Note that interpolation will not help to decoherent the fully coherent signals. Thanks to the process of interpolation, some decorrelation techniques can be applied to fully or partially recover the rank of the covariance matrix $\mathbf{\Gamma}$. In this paper, the forward-backward spatial smoothing (FBSS) method is considered with EPUMA [16] to partially recover the rank of the signal covariance matrix and enhance the final performance.

IV. MODIFIED EPUMA ALGORITHM

After the interpolation, $\mathbf{A}_l'$ approximates the Vandermonde structure, and the PUMA algorithm can be applied to estimate the real DOAs. The covariance matrix $\mathbf{\Gamma}$ in (15) can be written as

$$\mathbf{\Gamma} = \mathbf{A'}_l \mathbf{\Gamma}_s \mathbf{A'}_l^H \tag{16}$$

Then from (15) and (16),

$$\mathbf{A'}_l \mathbf{\Gamma}_s \mathbf{A'}_l^H = \mathbf{E}_{sl} \mathbf{D}_{sl} \mathbf{E}_{sl}^H \tag{17}$$

and

$$\mathbf{A'}_l \mathbf{T}\mathbf{T}^H \mathbf{A'}_l^H = \mathbf{E}_{sl} \mathbf{D}_{sl}^{1/2} \mathbf{D}_{sl}^{H/2} \mathbf{E}_{sl}^H \tag{18}$$

where $\mathbf{T} \in \mathbb{C}^{K \times N_r}$ and $\mathbf{D}_{sl}^{1/2} \in \mathbb{C}^{N_r \times N_r}$. From (18),

$$\mathbf{E}_{sl} = \mathbf{A'}_l \mathbf{T}_1 \tag{19}$$

where $\mathbf{T}_1 \in \mathbb{C}^{K \times N_r}$, (19) implies $span(\mathbf{E}_{sl}) = span(\mathbf{A'}_l \mathbf{T}_1)$.

So $\mathbf{A}_l'$ satisfies the following orthogonal relation obtained from the liner prediction theory [16]:

$$\mathbf{B}_T \mathbf{A}_l' = \mathbf{0} \tag{20}$$

where $\mathbf{B}_T \in \mathbb{C}^{(N-K) \times N}$ is a Toeplitz matrix, given by:

$$\mathbf{B}_T = \begin{bmatrix} c_K & c_{K-1} & \cdots & c_0 & 0 & \cdots & 0 & 0 \\ 0 & c_K & c_{K-1} & \cdots & c_0 & 0 & \cdots & 0 \\ \cdots & \cdots & \cdots & \ddots & \cdots & \cdots & \cdots & 0 \\ 0 & 0 & \cdots & 0 & c_K & c_{K-1} & \cdots & c_0 \end{bmatrix} \tag{21}$$

(21) reflects that for the k^{th} column in $\mathbf{A}'_l$, the $l^{th} \geq K+1$ row is a linear combination of the K previous rows, which can be expressed as

$$z_k^l + \sum_{i=1}^{K} c_i z_k^{l-i} = 0, K+1 \leq l \leq N; 1 \leq k \leq K \tag{22}$$

where $c_0 = 1$, $z_k = e^{j\pi \sin(\theta_k)}$. Now, the objective is to find the value of c_i, then the directions $\theta_1, ..., \theta_K$ can be obtained by the roots of the following polynomial of order K:

$$\sum_{i=0}^{K} c_i z^{K-i} = 0 \tag{23}$$

From (19) and (20),

$$\mathbf{B}_T \mathbf{A'}_l \mathbf{T}_1 = \mathbf{B}_T \mathbf{E}_{sl} = \mathbf{B}_T \left[\mathbf{u}_1, \mathbf{u}_2, \ldots, \mathbf{u}_{N_r}\right] = \mathbf{0}_{(N-K, N_r)} \tag{24}$$

thus, for the k^{th} column of $\mathbf{E}_{sl}$,

$$[\mathbf{u}_k]_l + \sum_{i=1}^{K} c_i [\mathbf{u}_k]_{l-i} = 0, \quad 1 \leq k \leq N_r; K+1 \leq l \leq N \tag{25}$$

Note that, as shown in (15) and (24), there are only N_r largest eigenvalues in $\mathbf{D}_{sl}$ in the case of multiple coherent sources. Therefore, the maximum value of k is not the number of sources K as used in [16], but the actual rank of the source covariance matrix N_r, which is the main distinctive difference between the proposed modified PUMA and the initial PUMA described in [16].

So (25) can be rewritten as follows:

$$\mathbf{F}_k \mathbf{c} - \mathbf{g}_k = \mathbf{0}_{(N-K,1)}, \quad 1 \leq k \leq N_r \tag{26}$$

where

$$\mathbf{F}_k = \begin{bmatrix} [\mathbf{u}_k]_K & [\mathbf{u}_k]_{K-1} & \cdots & [\mathbf{u}_k]_1 \\ [\mathbf{u}_k]_{K+1} & [\mathbf{u}_k]_K & \cdots & [\mathbf{u}_k]_2 \\ \vdots & \vdots & \ddots & \vdots \\ [\mathbf{u}_k]_{N-1} & [\mathbf{u}_k]_{N-2} & \cdots & [\mathbf{u}_k]_{N-K} \end{bmatrix}_{(N-K,K)}$$

$$\mathbf{g}_k = -\begin{bmatrix} [\mathbf{u}_k]_{K+1} \\ [\mathbf{u}_k]_{K+2} \\ \vdots \\ [\mathbf{u}_k]_N \end{bmatrix}_{(N-K,1)} \quad \mathbf{c} = \begin{bmatrix} c_1 \\ c_2 \\ \vdots \\ c_K \end{bmatrix}_{(K,1)} \tag{27}$$

and

$$\mathrm{vec}\left(\mathbf{B}_T \mathbf{E}_{sl}\right) = \mathbf{F}\mathbf{c} - \mathbf{g} = \mathbf{0}_{((N-K)N_r,1)} \tag{28}$$

where

$$\mathbf{F} = \begin{bmatrix} \mathbf{F}_1 \\ \mathbf{F}_2 \\ \vdots \\ \mathbf{F}_{N_r} \end{bmatrix}_{((N-K)N_r,K)} \quad \mathbf{g} = \begin{bmatrix} \mathbf{g}_1 \\ \mathbf{g}_2 \\ \vdots \\ \mathbf{g}_{N_r} \end{bmatrix}_{((N-K)N_r,1)} \tag{29}$$

In practice, with noise and limited samples, (26) is only an approximation. $\mathbf{c}$ can be obtained by the following weighted least squares (WLS) solution as proposed in [16]:

$$\hat{\mathbf{c}}_{WLS} = \left(\mathbf{F}^H \mathbf{W} \mathbf{F}\right)^{-1} \mathbf{F}^H \mathbf{W} \mathbf{g} \tag{30}$$

where $\mathbf{W} \cong \hat{\mathbf{T}} \otimes \left(\mathbf{B}_T \mathbf{B}_T{}^H\right)^{-1}$ and $\hat{\mathbf{T}}$ is a diagonal matrix defined as,

$$\hat{\mathbf{T}} = \mathrm{diag}\left(\lambda_1, \lambda_2, \ldots, \lambda_{N_r}\right) \tag{31}$$

It can be seen from (21) and (30) that the values of $\mathbf{W}$ and $\mathbf{c}$ depend on each other. Therefore, the modified PUMA is summarized in the following steps to obtain the K DOA estimates.

1. Calculate the initial $\mathbf{c}$ by the LS method: $\hat{\mathbf{c}} = \hat{\mathbf{c}}_{LS} = \left(\mathbf{F}^H \mathbf{F}\right)^{-1} \mathbf{F}^H \mathbf{g}$.
2. Calculate the weighting matrix $\mathbf{W}$ with $\hat{\mathbf{c}}$ by $\mathbf{W} \cong \hat{\mathbf{T}} \otimes \left(\mathbf{B}_T \mathbf{B}_T{}^H\right)^{-1}$ and (21), (31);
3. Calculate the $\hat{\mathbf{c}}_{WLS}$ with $\mathbf{W}$ by (30);
4. Determine whether $\|\hat{\mathbf{c}} - \hat{\mathbf{c}}_{WLS}\|_2$ becomes stable, if not let $\hat{\mathbf{c}} = \hat{\mathbf{c}}_{WLS}$, and repeat steps 2 and 3 until the stable criterion is satisfied, then obtain $\hat{\mathbf{c}}$.
5. Find the K roots $z_k = e^{j\pi \sin(\theta_k)}$ of the polynomial (23), then the K DOA candidates are obtained:

$$\hat{\theta}_k = \sin^{-1}\left(\frac{\angle \hat{z}_k}{\pi}\right), \quad k = 1, 2, \ldots, K \tag{32}$$

The modified EPUMA is a two-step DOA selection strategy of the modified PUMA based on the stochastic ML criteria, designed to improve the performance in scenarios with low signal-to-noise ratio (SNR) and/or coherent signals, while the initial EPUMA used the deterministic ML criteria for the analysis of simulation performance [16]. So the steps of the proposed modified EPUMA are summarized as follows,

1. Employ the modified PUMA algorithm twice, first with a source number of K and then with a supposed larger source number of P ($P >$ K), to generate $(K+P)$ DOA candidates.
2. Select the K DOA estimates from the $(K+P)$ DOA candidates based on the stochastic ML criteria as follows:

2.1.Divide $(K+P)$ DOAs into $G = \frac{(P+K)!}{K!P!}$ different groups with K DOAs in each group, represented by $\mathbf{\Theta}_1, ..., \mathbf{\Theta}_G$, corresponding to G different $\mathbf{A}'_l$, i.e., $\mathbf{A}'_l(\mathbf{\Theta}_1), ..., \mathbf{A}'_l(\mathbf{\Theta}_G)$;

TABLE 1. DOA Estimation Algorithm for Coherent Signals Based on the Modified EPUMA Method with FBS-LWA

Algorithm 1: DOA Estimation of Coherent Signals Based on the Modified EPUMA Method with FBS-LWA
1. Obtain $\mathbf{y}$ by the received the signals after FFT.
2. Obtain the approximate range of incident angles by the corresponding frequencies of the peaks of the received signal power spectrum and radiation patterns and/or utilizing the beamforming method.
3. Adopt the uniform distribution to get the virtual directions $\theta_1, \theta_2, \ldots, \theta_{K_v}$.
4. Determine the $\mathbf{A}_r$ and $\mathbf{A}_l$ with virtual directions by (7) and (8), respectively.
5. $\mathbf{A}_r$ and $\mathbf{A}_l$ are applied to get the interpolation matrix $\mathbf{B}_i$ by (9)-(11).
6. Obtain $\mathbf{y}_l$ by (12) with $\mathbf{B}_i$, (13)-(15) are applied to obtain the covariance matrix $\mathbf{\Gamma}$.
7. Decompose $\mathbf{\Gamma}$ by (15), then obtain the estimated DOAs via the modified EPUMA by (16)-(33).

2.2. Calculate the stochastic ML cost function $L(\mathbf{\Theta}_i)$ of each $\mathbf{A}'_l(\mathbf{\Theta}_i)$, $i \in \{1, \ldots, G\}$;

$$L(\mathbf{\Theta}_i) = log\left\{\det\left(\mathbf{P}_{\mathbf{A}'_l}\mathbf{\Gamma}\mathbf{P}_{\mathbf{A}'_l} + \frac{tr\left(\mathbf{P}^{\perp}_{\mathbf{A}'_l}\mathbf{\Gamma}\right)\mathbf{P}^{\perp}_{\mathbf{A}'_l}}{N-K}\right)\right\} \tag{33}$$

with $\mathbf{P}_{\mathbf{A}'_l} = \mathbf{A}'_l(\mathbf{\Theta}_i)(\mathbf{A}'^{\mathrm{H}}_l(\mathbf{\Theta}_i)\mathbf{A}'_l(\mathbf{\Theta}_i))^{-1}\mathbf{A}'^{\mathrm{H}}_l(\mathbf{\Theta}_i)$, and $\mathbf{P}^{\perp}_{\mathbf{A}'_l} = \mathbf{I}_N - \mathbf{P}_{\mathbf{A}'_l}$.

2.3 Choose the group $\mathbf{\Theta}_i$ with minimum $L(\mathbf{\Theta}_i)$.

Compared to the classical EPUMA, the modified EPUMA can handle the rank deficiency of the source covariance matrix due to the multiple coherent signals with reduced computational load by replacing K with N_r (the actual rank of noise free sources covariance matrix). Note, after preprocessing by FBSS method, $N_r = 2$ for the fully multiple coherent sources when $K \geq 2$.

The steps of DOA estimation of coherent signals based on the modified EPUMA method with FBS-LWA are summarized in Table I.

V. SIMULATION RESULTS OF DOA ESTIMATION WITH COHERENT SIGNALS

In this section, some simulation results of DOA estimation of coherent signals via the proposed modified EPUMA based on interpolated FBS-LWA signal model are provided. Unless stated otherwise, the parameters of FBS-LWA are the same as in Figure 2 (a), $l = 20$ cm and $\alpha_n/k_{0n} = 0.01$ with 200 frequency samples from $f_{min} = 24$ GHz to $f_{max} = 36$ GHz in the subsequent simulations. The probabilities of source detection P_r is calculated by $P_r = I_s/I$, where I_s represents the number of successful estimations of sources, and I represents the number of Monte Carlo iterations. When

$$\left|\hat{\theta}_i - \theta_i\right| < \frac{\Delta\theta}{2}, i = 1, 2, \ldots, K \tag{34}$$

is met, it counts a successful estimation of sources, where $\Delta\theta = \min|\theta_m - \theta_n|, 1 \leq n < m \leq K$, and $\hat{\theta}_i$ is the estimated angle of θ_i. The root-mean-square error (RMSE), which is used to assess the performance of the proposed method, is defined by

$$\mathrm{RMSE} = \left(\frac{1}{KI}\sum_{k=1}^{K}\sum_{i=1}^{I}\left(\hat{\theta}_{k,i} - \theta_k\right)^2\right)^{1/2} \tag{35}$$

where $\hat{\theta}_{k,i}$ is the k^{th} estimated angle obtained from the i^{th} test and θ_k is the k^{th} true angle. Unless stated otherwise, the number of Monte Carlo tests is 100, and the number of snapshots is 200. And MUSIC is combined with MSSP including 10 overlapping subarrays, each subarray consists of 190 elements.

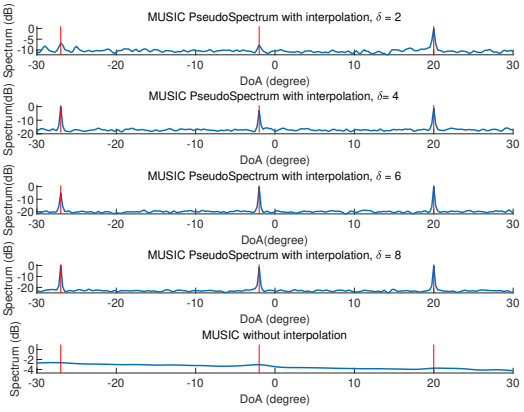

FIGURE 3. MUSIC Pseudo-spectrum versus θ with three coherent signals from directions $-27°$, $-2°$, $20°$, $\theta_{B,k} = \theta_k$, and SNR = 7dB.

In uniform distribution, assuming that the interpolation interval δ in each sector is $2, 4, 6, 8$ respectively, and $\theta_{B,k} = \theta_k, k = 1, 2, \ldots, K'$. If there are too many virtual directions, the matrix $\mathbf{A}_r$ will be ill-conditioned. It has been found empirically that $p = 1$ yields the best result with the LWA model used in this paper.

As an illustration, MUSIC is firstly applied (i) directly on the received estimated covariance matrix $\mathbf{R}$ and (ii) on the interpolated and MSSP-processed estimated covariance matrix and examples of Pseudo-spectrum are given in Figure 3. Three coherent signals coming from $[-27°, -2°, 20°]$ with SNR = 7dB are used in the simulation. It is obvious that the classical MUSIC (without interpolation) shows the worst result while the pseudo-spectral of MUSIC with $\delta = 6$ has a dynamic range around 18dB. This confirms the effectiveness of the proposed interpolation procedure combined with MSSP to estimate the DOA of coherent sources with FBS-LWA.

As shown in Figure 4, the proposed modified EPUMA is applied with the interpolation method with two coherent signals coming from $[-1.5°, 2.5°]$, where $\theta_{B,k} = \theta_k + \theta_{random,k}$. $\theta_{random,k}$ obeys a uniform distribution of $[0°, 6°]$, which represents the possible estimation errors

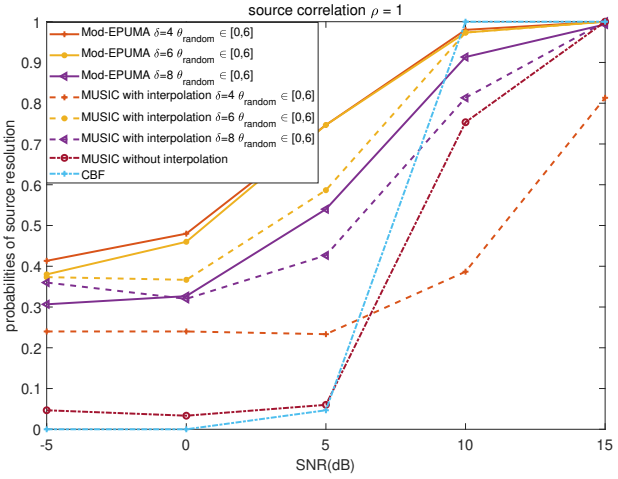

FIGURE 4. Probabilities of source detection versus SNR with two coherent signals from directions -1.5°, 2.5°, $\theta_{B,k} = \theta_k + \theta_{random,k}$.

of a prior approximate DOA in (6). And the number of Monte Carlo tests in the simulation is 150. For various values of δ, the probabilities of source detection of the proposed modified EPUMA are mostly higher than those obtained by MUSIC with and without interpolation, which illustrates the better performance of the proposed modified EPUMA. Note that, with some parameters, especially in the case of low SNR, the classical MUSIC and classical beamforming method (CBF) can only identify fewer spectrum peaks than the number of sources, which causes relatively large errors and low resolution.

The proposed method, i.e., the algorithm in Table 1, is applied to three coherent signals coming from $[-27^\circ, -2^\circ, 20^\circ]$ and the obtained results are shown in Figure 5. In Figure 5(a) and Figure 5(b), the comparison between different numbers of frequency samples is performed. In Figure 5(a), the number of frequency samples is 200, while in Figure 5(b), it is 100. In Figure 5(a), the RMSE of the proposed method exhibits a rapid decrease when SNR exceeds 10 dB, with the effect of δ becoming more pronounced. When the number of frequency samples is reduced, there is a slight degradation in the accuracy of the proposed method. The RMSE of the proposed method decreases rapidly when SNR is greater than 10 dB. The impact of different numbers of frequency samples on the proposed algorithm is not significant, as long as the maximum and minimum frequencies remain unchanged. Notably, when $\delta = 6$, the RMSE performance is superior compared to other values, as it leads to a better conditioned $\mathbf{A}_\tau$. On the other hand, the classical MUSIC shows the poorest RMSE performance.

The difference between Figure 5(a) and Figure 5(c) is the value of the length l of LWA, $l = 20$ cm in Figure 5(a), while $l = 10$ cm in Figure 5(c). In Figure 5(c),

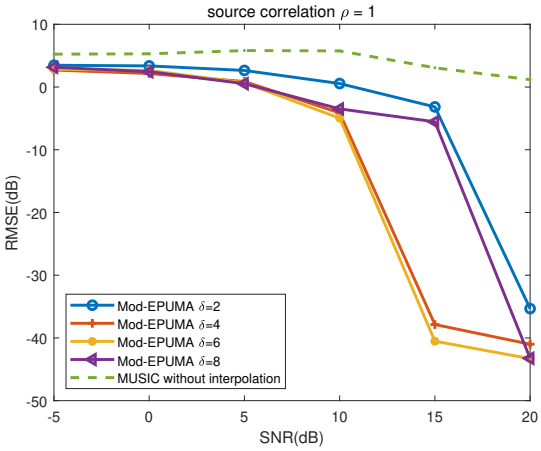

(a) 200 frequency samples, $l = 20$ cm.

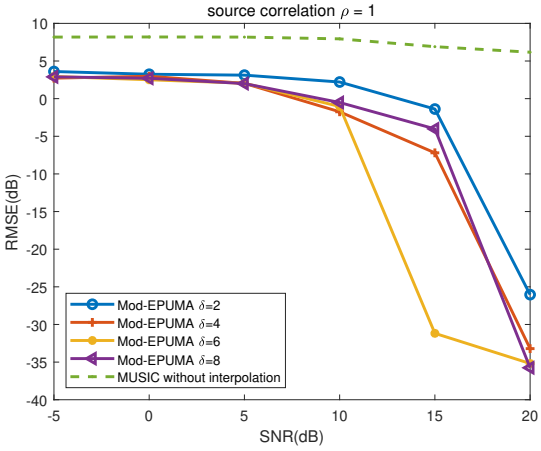

(b) 100 frequency samples, $l = 20$ cm.

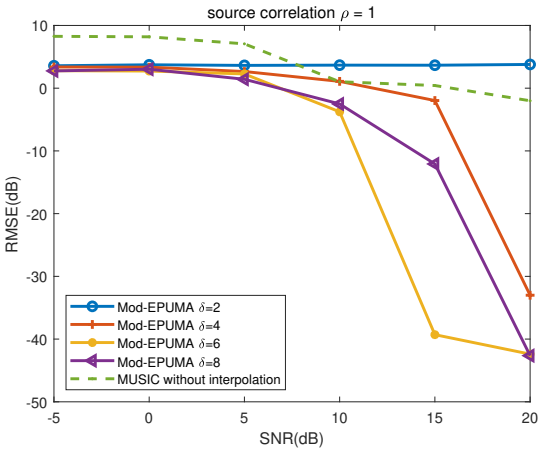

(c) 200 frequency samples, $l = 10$ cm.

FIGURE 5. RMSE performance versus SNR by uniform distribution with three coherent signals from directions -27°, -2°, 20°, $\theta_{B,k} = \theta_k$.

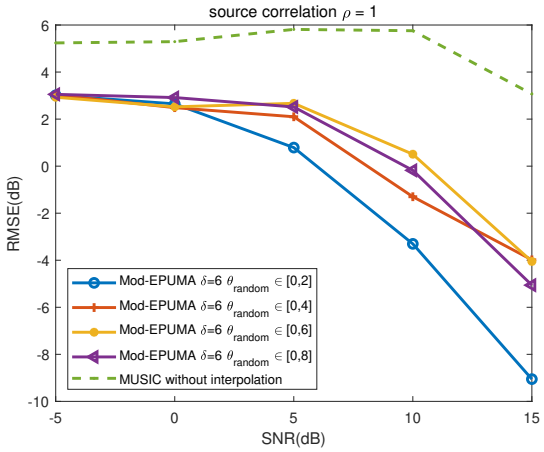

(a) RMSE performance versus SNR

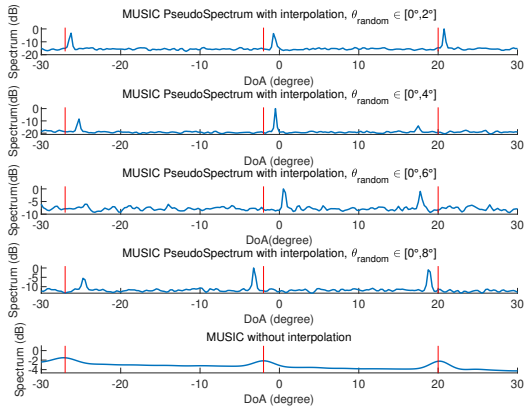

(b) MUSIC performance with SNR=7 dB

FIGURE 6. DOA estimation by uniform distribution with three coherent signals from directions $-27°$, $-2°$, $20°$, $\theta_{B,k} = \theta_k + \theta_{random,k}$

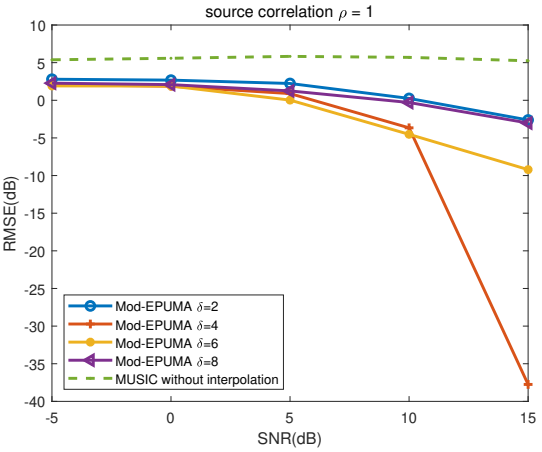

(a) RMSE performance versus SNR

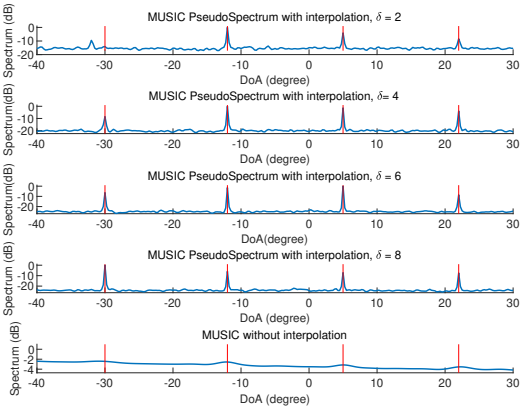

(b) MUSIC performance with SNR=7 dB

FIGURE 7. DOA estimation by uniform distribution with four coherent signals from directions $-30°$, $-12°$, $5°$,$22°$, $\theta_{B,k} = \theta_k$

the best RMSE performance is obtained when $\delta = 6$, which is similar to the situation in Figure 5(a). And for the same δ, the length l impacts the RMSE performance slightly. So by this simulation, it can conclude that the proposed method is robust for different values of the length l. Moreover, due to the wider beamwidth when $l = 10$ cm as shown in Figure 2, the DOA estimation can be performed by incorporating a suitable number of interpolation points and/or a fitting interpolation interval δ, adapted to the beamwidth of each radiation pattern of FBS-LWA, to achieve a comparable RMSE performance.

As shown in Figure 6, the simulations with three coherent signals coming from $[-27°, -2°, 20°]$ are performed, where $\theta_{B,k} = \theta_k + \theta_{random,k}$. $\theta_{random,k}$ obeys a uniform distribution of $[0°, 2°]$, $[0°, 4°]$, $[0°, 6°]$ and $[0°, 8°]$, respectively, which are compared with each other for $\delta = 6$ and 200 frequency samples. In Figure 6(a), $\theta_{random,k} \in [0°, 2°]$ have the best RMSE performance, but the minimum RMSE changes from -40.5 dB in Figure 5 to -9 dB at SNR $= 15$ dB. Compared with Figure 5, although there are some errors in the approximate DOAs, the uniformly distributed interpolation method still provides precise DOAs. In Figure 6(b), although MUSIC with interpolation superiors classical MUSIC, the accuracy is reduced due to the effect of $\theta_{random,k}$ compared to Figure 3.

Simulation results with four coherent signals with respective DOAs $[-30°, -12°, 5°, 22°]$ are shown in Figure 7. In Figure 7(a), the best performance and accuracy are achieved when $\delta = 4$, which implies that the proposed algorithm can perform reliable estimation, while the other situation corresponds to an improvement of less than about 10 dB. Besides, as the number of sources increases, the advantage of interpolation becomes more apparent. Even in the case of $\delta = 2$, there is a significant advantage. In Figure 7(b), the performance of MUSIC is similar to Figure 3. Regardless of the algorithm, interpolation makes its performance better in this scenario.

The RMSE performance versus the number of sources K for the proposed method with SNR $= 20$ dB is

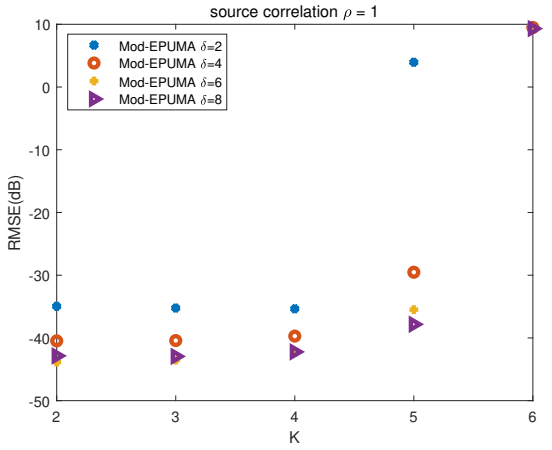

FIGURE 8. RMSE performance versus the number of sources by uniform distribution with $\theta_{B,k} = \theta_k$

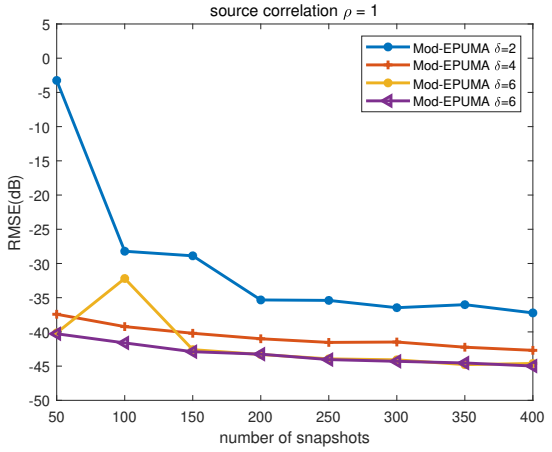

FIGURE 9. RMSE performance versus the number of snapshots with three coherent signals with DOAs of $-27°$, $-2°$, $20°$, $\theta_{B,k} = \theta_k$

shown in Figure 8. The RMSE values of the proposed method gradually increase with increasing K. When $K \leq 4$, $\delta = 6$ can obtain reliable performance, which is corresponding to the performance of Figure 5. However, when $K = 5$, the RMSE value with $\delta = 2$ rises rapidly, and when $K = 6$, the RMSE value is around 10 dB regardless of the value of δ, which means when $K \geq 6$, the true DOAs of the multiple coherent signals cannot be obtained effectively by the proposed method.

The RMSE performance versus the number of snapshots for the proposed method with three coherent signals coming from $[-27°, -2°, 20°]$ and SNR = 20 dB is shown in Figure 9. The RMSE value of the proposed method gradually decreases as the number of snapshots increases when $\delta = 2$. And for other values of δ, the proposed method achieves reliable performance even for small snapshots.

VI. CONCLUSION

Thanks to its frequency beam scanning characteristic, leaky-wave antenna (LWA) can drastically decrease DOA estimation system complexity. This paper proposes a DOA estimation method of multiple coherent signals by a combination of a modified EPUMA algorithm and an interpolation technique with a FBS-LWA. To satisfy the requirement of EPUMA algorithm, the steering matrix of the FBS-LWA is transformed into a virtual Vandermonde matrix by interpolation technique. The proposed modified EPUMA algorithm is then applied to handle the rank-deficient case owing to multiple coherent signals. The proposed method can be extended to other types of non-uniform distributed antennas for DOA estimation of coherent signals. Simulation results show that the DOA of coherent sources, which can model the multipath phenomena in wireless communication, can be effectively estimated. For instance, with 3 coherent sources impinging on the LWA, an RMSE of less than -36 dB for a 15 dB SNR is achieved using 200 frequency samples and 200 snapshots.

Note that the interpolation technique is utilized to transform the actual steering matrix into a virtual Vandermonde structured steering matrix for decorrelation preprocessing, which results in an increase of the computational complexity due to the calculation of the interpolation matrix. Additionally, the knowledge of the approximate angles $\mathbf{\Theta}_B$ is necessary to generate the K_v virtual angles using (6) in order to construct $\mathbf{A}_r$ using (7). This a priori knowledge can be simply determined from the power spectrum of the received signal directly using (5). Thus, the proposed method is specifically suitable for single-beam FBS-LWA. Future research efforts will focus on developing low computational complexity DOA estimation methods for coherent signals received by multibeam FBS-LWA.

REFERENCES

[1] M. Poveda-García, D. Cañete-Rebenaque and J. L. Gómez-Tornero, "Frequency-Scanned Monopulse Pattern Synthesis Using Leaky-Wave Antennas for Enhanced Power-Based Direction-of-Arrival Estimation," *IEEE Trans. Antennas Propag.*, vol. 67, no. 11, pp. 7071-7086, 2019.

[2] A. A. Hussain, N. Tayem, A. -H. Soliman and R. M. Radaydeh, "FPGA-Based Hardware Implementation of Computationally Efficient Multi-Source DOA Estimation Algorithms," *IEEE Access*, vol. 7, pp. 88845-88858, 2019.

[3] N. Javanbakht, B. Syrett, R. E. Amaya and J. Shaker, "A Review of Reconfigurable Leaky-Wave Antennas," *IEEE Access*, vol. 9, pp. 94224-94238, 2021.

[4] D. R. Jackson, C. Caloz and T. Itoh, "Leaky-Wave Antennas," *Proceedings of the IEEE*, vol. 100, no. 7, pp. 2194-2206, 2012.

[5] D. Zheng, C. H. Chan and K. Wu, "Leaky-Wave Structures and Techniques for Integrated Front-End Antenna Systems," *IEEE Journal of Microwaves*, vol. 3, no. 1, pp. 368-397, 2023.

[6] X. Yu and H. Xin, "Direction of arrival estimation utilizing incident angle dependent spectra," in *Proc. IEEE/MTT − S Int. Symp. Diget Microwave*, Montreal, QC, Canada, 2012, pp. 1-3.

[7] H. Paaso, A. Mämmelä, D. Patron and K. R. Dandekar, "DoA estimation through modified unitary MUSIC algorithm for CRLH leaky-wave antennas," in *Proc. IEEE Int. Symp. on Personal, Indoor, and Mobile Radio Commun.* (*PIMRC*), London, UK, 2013, pp. 311-315.
[8] H. Paaso et al., "DoA Estimation Using Compact CRLH Leaky-Wave Antennas: Novel Algorithms and Measured Performance," *IEEE Trans. Antennas Propag.*, vol. 65, no. 9, pp. 4836-4849, Sept. 2017.
[9] J. Sarrazin, "MUSIC-based Angle-of-Arrival Estimation using Multi-beam Leaky-Wave Antennas," in *XXXIVth General Assembly and Scientific Symp. Int. Union of Radio Science* (*URSIGASS*), Rome, Italy, 2021, pp. 1-4.
[10] M. Poveda-García, et al., "RSSI-based direction-of-departure estimation in bluetooth low energy using an array of frequency-steered leaky-wave antennas", *IEEE Access*, vol. 8, pp. 9380-9394, Jan. 2020
[11] A. Gil-Martínez, et al., "Wi-Fi direction finding with frequency-scanned antenna and channel-hopping scheme," *IEEE Sensor Journal*, vol. 22, no. 6, pp. 5210-5222, Mar. 2022
[12] A. Gil-Martínez, et al., "Direction finding of RFID tags in UHF band using a passive beam-scanning leaky-wave antenna", *IEEE Journal of Radio Frequency Identification*, vol. 6, pp. 552-563, Jun. 2022.
[13] J. Sarrazin, G. Valerio, "Multibeam Leaky-Wave Antenna for Mm-wave Wide-Angular-Range AoA Estimation", *16th European Conference on Antennas and Propagation* (*EuCAP*), Madrid, Spain, 27 March-1st April 2022
[14] J. Sarrazin, G. Valerio, "H-Plane-Scanning Multibeam Leaky-Wave Antenna for Wide-Angular-Range AoA Estimation at mm-wave", *17th European Conference on Antennas and Propagation* (*EuCAP*), Florence, Italy, 26-31 March 2023
[15] J. Pan, M. Sun, Y. Wang and X. Zhang, "An Enhanced Spatial Smoothing Technique With ESPRIT Algorithm for Direction of Arrival Estimation in Coherent Scenarios," *IEEE Trans. Signal Process.*, vol. 68, pp. 3635-3643, 2020.
[16] C. Qian, L. Huang, N. D. Sidiropoulos, and H. C. So, "Enhanced PUMA for direction-of-arrival estimation and its performance analysis," *IEEE Trans. Signal Process.*, vol. 64, no. 16, pp. 4127–4137, 2016.
[17] B. Tchana Tankeu, V. Baltazart, Y. Wang, D. Guilbert, "PUMA Applied to Time Delay Estimation for Processing GPR Data over Debonded Pavement Structures," *Remote Sensing*, vol. 13, no. 17, 3456, 2021.
[18] Z. Zheng, Y. Huang, W. -Q. Wang and H. C. So, "Direction-of-Arrival Estimation of Coherent Signals via Coprime Array Interpolation," *IEEE Signal Process. Lett.*, vol. 27, pp. 585-589, 2020.
[19] S. Xu, D. Guan, et al.,"A Wide-Angle Narrow-Band Leaky-Wave Antenna Based on SIW-SPP Structure," *IEEE Antennas Wireless Propag. Lett.*, vol.18, no. 7, pp. 1386-1389, 2019.
[20] L. Jidi, X. Cao, J. Gao, et al., "Ultrawide-Angle and High-Scanning-Rate Leaky Wave Antenna Based on Spoof Surface Plasmon Polaritons," *IEEE Trans. Antennas Propag.*, vol.70, no. 3, pp. 2312-2317, 2022.

DIYUAN XU received the B.S. degree in railway traffic signaling and control from Southwest Jiaotong University, Chengdu, China, in 2020. She received the M.S. degree in wireless embedded technologies from the University of Nantes, France, in 2022. She is currently pursuing the M.S. degree in information engineering with South China University of Technology, Guangzhou, China. Her research interests include array signals processing and wireless communication.

YIDE WANG received the B.S. degree in electrical engineering from the Beijing University of Post and Telecommunication, Beijing, China, in 1984, and the M.S. and the Ph.D. degrees in signal processing and telecommunications from the University of Rennes, France, in 1986 and 1989, respectively. He is currently a Professor with the Ecole Polytechnique de Nantes Université. His research interests include array signal processing, signal processing for fault detection and diagnosis in electrical machines.

JULIEN SARRAZIN received his Master and PhD degrees from the University of Nantes in France, in 2005 and 2008 respectively. In 2009 and 2010, he worked with the BK Birla Institute of Technology of Pilani, India. In 2011 and 2012, he was a research engineer at Telecom ParisTech in Paris. Since September 2012, he is an Associate Professor at Sorbonne Université in Paris. His research interests include antenna design, spatial data focusing and channel modeling.

BIYUN MA received the B.S. degree in information engineering from the South China University of Technology, Guangzhou, China, in 2004, and the M.S. and the PH.D. degrees in electronic engineering from the Nantes University, France, in 2007 and 2010 respectively. She is currently an associate professor with the School of Electronic and Information Engineering of South China University of Technology. Her research interests include array signal processing, mobile wireless communication systems, signal processing for ultrasonic detection and communication.

QINGQING ZHU received the B.S. degree in Information Engineering in 2022 and is currently working toward the M.S. degree in Electronic Information from South China University of Technology, GuangZhou, China. Her current research interests include array signal processing, spectral estimation and signal processing for communications.